

Simulating the Reactions of CO₂ in Aqueous Monoethanolamine Solution by Reaction Ensemble Monte Carlo Using the Continuous Fractional Component Method

Sayee Prasaad Balaji,[†] Satesh Gangarapu,[‡] Mahinder Ramdin,[†] Ariana Torres-Knoop,[¶] Han Zuilhof,^{‡,§} Earl L.V. Goetheer,[¶] David Dubbeldam,[¶] and Thijs J.H. Vlugt^{*,†}

[†]Engineering Thermodynamics, Process & Energy Department, Faculty of Mechanical, Maritime, and Materials Engineering, Delft University of Technology, Leeghwaterstraat 39, 2628CB Delft, The Netherlands

[‡]Laboratory of Organic Chemistry, Wageningen University, Dreijenplein 8, 6703HB Wageningen, The Netherlands

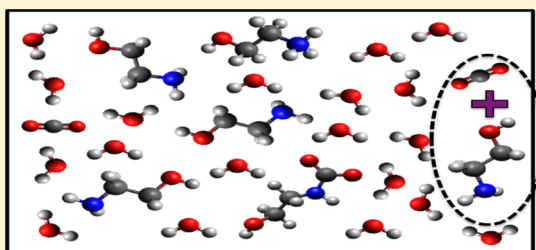
[¶]Van't Hoff Institute for Molecular Sciences, University of Amsterdam, Science Park 904, 1098XH Amsterdam, The Netherlands

[§]Department of Chemical and Materials Engineering, King Abdulaziz University, Jeddah, Saudi Arabia

[¶]TNO, Leeghwaterstraat 46, 2628CA Delft, The Netherlands

S Supporting Information

ABSTRACT: Molecular simulations were used to compute the equilibrium concentrations of the different species in CO₂/monoethanolamine solutions for different CO₂ loadings. Simulations were performed in the Reaction Ensemble using the continuous fractional component Monte Carlo method at temperatures of 293, 333, and 353 K. The resulting computed equilibrium concentrations are in excellent agreement with experimental data. The effect of different reaction pathways was investigated. For a complete understanding of the equilibrium speciation, it is essential to take all elementary reactions into account because considering only the overall reaction of CO₂ with MEA is insufficient. The effects of electrostatics and intermolecular van der Waals interactions were also studied, clearly showing that solvation of reactants and products is essential for the reaction. The Reaction Ensemble Monte Carlo using the continuous fractional component method opens the possibility of investigating the effects of the solvent on CO₂ chemisorption by eliminating the need to study different reaction pathways and concentrate only on the thermodynamics of the system.



1. INTRODUCTION

Carbon dioxide (CO₂) is the most important greenhouse gas present in combustion flue gases. It accounts for an abundant portion of the emitted greenhouse gases.^{1,2} The capture of CO₂ from flue gases, its transport, and storage has been identified to be of crucial importance to reduce the carbon footprint in the atmosphere.³ Postcombustion CO₂ capture processes are particularly important for power plants operating on fossil fuels, such as coal, natural gas, and so forth, as they contribute ~25% of global CO₂ emissions.^{4,5} Scientific progress has contributed to the rapid growth of industries, and this has drastically increased the demand for energy. This translates to an increased dependency on fossil fuels, because alternate energy sources have not yet been fully developed.⁶ To reduce CO₂ emissions into the atmosphere, it is necessary to capture CO₂ from flue gas streams. Typically, the removal of CO₂ from flue gas streams is carried out using liquid amine solvents.⁷ Monoethanolamine-containing (MEA) solutions were among the first alkanolamine-based solvents used in the capture of CO₂. This system remains one of the most important solvents in postcombustion CO₂ capture.⁸ Some of the advantages of using MEA solutions for CO₂ capture are the high CO₂

absorption capacity and reaction rates and low cost of solvents.^{6,8} To regenerate the solvent, heat must be supplied.^{6,8,9} Some of the disadvantages of using MEA solution as solvents include the high energy demand to regenerate the solvent and emissions of MEA solvents as aerosols.^{10,11} MEA solutions are also susceptible to oxidative and thermal degradation.^{10–12}

The mechanism of CO₂ absorption in MEA solutions is chemical in nature. CO₂ reacts with the MEA solution to form stable carbamates.^{7–9,13,14} To study the chemisorption of CO₂ in MEA solutions and to reduce the heat required to regenerate the alkanolamine after CO₂ capture, it is necessary to study the chemical reactions that take place in the solution.¹⁴ There are several possible mechanisms to explain how CO₂ reacts with alkanolamines.^{9,14–16} CO₂ reacts through an acid–base buffer mechanism with the alkanolamines to form protonated amines. CO₂ also reacts with some primary and secondary alkanolamines to form carbamates and reacts with tertiary alkanolamines to form bicarbonates.^{9,14,15} To design a CO₂ amine

Received: February 19, 2015

Published: May 8, 2015



treating process, it is important to understand the chemical equilibrium as well as the kinetics of the different reactions. There are many studies in the literature about the CO₂/MEA system.^{7,10,17,18} Sartori and Savage obtained equilibrium constants for carbamate formation.¹⁹ Batt et al.²⁰ and Maddox et al.²¹ qualitatively investigated the reactions that occur in the MEA system. Poplsteinova et al.²² have studied systems containing MEA and *N*-methyl-diethanolamine using NMR spectroscopy. Hasse and co-workers⁹ have studied the chemical equilibria of CO₂ in aqueous alkanolamines using online NMR spectroscopy. Chemical equilibria and kinetics of CO₂/alkanolamine solutions are difficult to study experimentally at the molecular level because of the extremely fast reaction rates and different reaction mechanisms.

Molecular simulations play an important role in bridging the gap between our understanding of reaction phenomena on a molecular level and experimental observations on a macroscopic scale.²³ The impact of individual reactions and reaction mechanisms on the chemical equilibrium of a system can be studied using molecular simulations. Quantum chemical methods are widely applied to compute stationary points on the potential energy surface, such as transition states and activation barriers. Time dependent *ab initio* methods like Car–Parrinello molecular dynamics²⁴ can be used to model the reactions directly. These methods scale poorly with system size and are sometimes difficult to apply to liquid phases. A classical-based approach developed by Van Duin et al. uses “Reactive” force fields (ReaxFF) that are parametrized to study the chemical reactions of a few systems using classical molecular dynamics simulations.²⁵ ReaxFF treats the intermolecular interactions between the atoms and molecules through a classical force field that has been parametrized from experimental data or quantum simulations.²⁵ Another classical-based approach called the Reaction Ensemble Monte Carlo (RxMC) for studying chemical reactions in equilibrium ignores transient events like bond breaking and formation (reaction mechanisms in general). This approach is ideal for studying the equilibrium distributions of the reacting species, because the effect of the intermolecular interactions with the surrounding molecules are taken into account. It is important to realize that equilibrium speciation is determined by the thermodynamics of the system, for which classical molecular simulations are a suitable tool. The RxMC was developed independently by Johnson et al.²⁶ and Smith and Triska.²⁷ An important feature of RxMC is the actual reaction. Its transition path is not simulated; only the equilibrium configurations of the molecules before and after the reaction are sampled. The forward and backward reactions are sampled using stochastic trial moves. In the case of a forward reaction, the reactant molecules are chosen at random and are deleted from the simulation box while the product molecules are inserted randomly according to the stoichiometry of the reaction. This RxMC method requires the input of stoichiometric coefficients of the reactants and products and the ideal gas partition functions of isolated reactant and product molecules along with the intermolecular potential parameters to describe the interactions between the molecules. These ideal gas partition functions of isolated molecules can be obtained from thermophysical tables or quantum mechanical calculations.^{28–30}

The partition function of ideal gas molecules depends on the volume of the simulation box and must be taken into account in the acceptance rules of the RxMC algorithm (see the Supporting Information for details).

Previous research pertaining to RxMC has focused on small molecules with fixed internal degrees of freedom.^{26,27,31–34} Lisal and co-workers^{35,36} have developed the Reaction Ensemble Monte Carlo for systems with flexible internal degrees of freedom to study the synthesis of methyl-*tert*-butyl-ether (MTBE) from isobutene and methanol. The acceptance rules for the reaction move derived by Lisal and co-workers also include the change in energy due to intramolecular contributions. Intermolecular interactions are counted twice in their derivation of the acceptance rules, which is incorrect.^{30,35,36} Rosch et al.³⁰ have derived the correct acceptance rules. Keil et al.^{28,29} have studied propene metathesis reactions within confined environments. These authors have combined the configurational-bias Monte Carlo (CBMC) approach with the RxMC for linear alkanes and alkenes. The CBMC algorithm is useful for simulating larger molecules, because inserting these large molecules in confined systems is extremely difficult. To the best of our knowledge, application of the RxMC for complex molecules and reactions in a dense liquid phase has not been studied.

A reaction in the Reaction Ensemble involves the deletion of reactants and the insertion of the reaction products. These so-called “insertions” and “deletions” are accepted in such a way that the correct equilibrium distribution is sampled. The efficiency and accuracy of these simulations depend on the probability of successful insertions and deletions of the molecules. At the high densities typically encountered in a liquid phase, the probability of successful insertions and deletions is very low due to a large number of overlaps with existing molecules in the simulation box.^{23,37,38} To increase the efficiency of successful insertions and deletions, Maginn et al.^{37,39} have developed the continuous fractional component Monte Carlo (CFCMC) method to insert/delete molecules in a more gradual manner. Torres-Knoop et al.³⁸ have combined the CBMC with the CFCMC to obtain higher computational efficiencies. Other works have been published proposing methods that try to increase the efficiency of insertions and deletions in dense liquids.^{40–42} Rosch et al. have extended the CFCMC method for the Reaction Ensemble, coupling the CFCMC for inserting the product molecules and deleting the reactant molecules based on their respective stoichiometry.³⁰

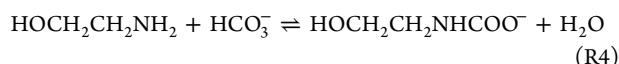
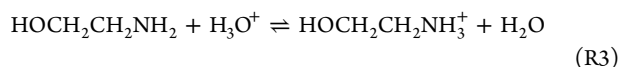
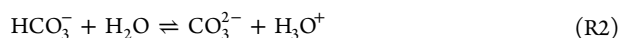
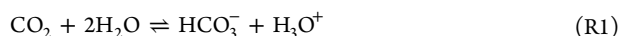
In this work, we use the Reaction Ensemble Monte Carlo using the continuous fractional component (RxMC/CFC) method to study the chemical equilibrium of CO₂ in MEA solution and to determine the equilibrium concentrations of the different species in the system. The results are compared to experimental results from the literature. We study the effects of different reaction mechanisms on the equilibrium concentrations of the various species. The rest of this paper is organized as follows: section 2 deals with simulating the reactions of CO₂ in MEA solution along with derivation of the acceptance rules for the RxMC/CFC algorithm, and section 3 contains the different results, discussion, and summary of our findings from section 2.

2. SIMULATING THE REACTIONS OF CO₂ IN MONOETHANOLAMINE SOLUTION

The reactions of CO₂ with primary and secondary amine solutions usually take place through an acid–base buffer mechanism, which results in the formation of stable carbamates and bicarbonate followed by the subsequent protonation of the amine.²¹ Nonhindered primary and secondary amines react rapidly with CO₂ to form carbamate ions, and the addition of

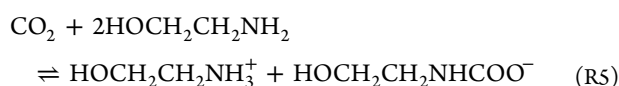
water increases the absorption capacity and rate. Tertiary amines react with CO_2 via the bicarbonate pathway to form a bicarbonate ion and the ammonium salt of the amine. Because monoethanolamine ($\text{HOCH}_2\text{CH}_2\text{NH}_2$) is a primary amine, the reactions take place via the carbamate ion pathway:^{14,15}

MEA + CO_2 (carbamate pathway) reactions:



These reactions are generally described in the literature.^{9,14,15,22}

It is important to note that, in the reactions mentioned above, the appearance of H_3O^+ is to avoid the presence of H^+ in the system, because H^+ does not obey the Born–Oppenheimer approximation for classical simulations.²³ Some other additional reactions have also been described in the literature.⁹ MEA is also able to form 2-oxazolidone, which is a heterocyclic component.^{9,43} Other amine degradation reaction mechanisms are also possible.^{43,44} In spite of the different possible reaction mechanisms, the aim of all modeling and experimental studies is to obtain the equilibrium concentrations of the different species. In this regard, reactions R1, R3, and R4 may be combined to result in the simplified reaction R5, which is given by



2.1. RxMC/CFC Algorithm. To obtain the equilibrium concentrations of the different species in a reacting mixture, we used the Reaction Ensemble Monte Carlo (RxMC).^{26,28,29,45} The RxMC algorithm samples the reactions directly and bypasses transition states. The RxMC algorithm only requires the stoichiometric coefficients of the reactions as an input and the partition functions of the isolated molecules or ions, along with the force field parameters, to compute the intermolecular interactions. Therefore, the RxMC method allows for a systematic study of the effect of the medium (or solvent) on the reaction equilibrium constant.

The reaction trial move within the RxMC framework involves choosing the forward or reverse reaction at random. If the forward reaction is chosen, the reactant molecules are deleted, and the product molecules are inserted according to their stoichiometries. For dense systems, these insertions and deletions of molecules, if performed in a single step, often lead to overlaps with the surrounding molecules. The probabilities of successful insertions/deletions of the molecules are very low. To circumvent this problem, Maginn et al.^{37,39} have developed the continuous fractional component Monte Carlo method. Fractional molecules of the reactants and products are introduced into the system. By controlling the interactions of these fractional molecules with their surrounding molecules, the reactants/products are gradually inserted or removed. This is controlled by a pseudocoupling factor (λ). Changes in λ will gradually insert or delete the molecules appropriately.

The reaction ensemble is best described by taking the osmotic ensemble as the starting point because most chemical reactions take place in a system at constant pressure. Let N_i

denote the number of molecules of type i , P the imposed hydrostatic pressure, V the volume, and μ_i the chemical potential of species i . For an expanded osmotic ensemble, the partition function for a system of n species can be expressed as³⁰

$$\begin{aligned} \Xi_{\text{biased}}(\mu_1, \dots, \mu_n, p, T) \\ = \beta P \int_0^1 d\lambda \sum_{N_i=0}^{\infty} \dots \sum_{N_n=0}^{\infty} \int \exp \left[\beta \sum_{i=1}^n N_i \mu_i - \sum_{i=1}^n \ln N_i! \right. \\ \left. + \sum_{i=1}^n N_i \ln(\hat{q}_i(T)V) - \beta PV - \beta U(s^N, \omega^N, \lambda) \right] \\ \exp[\eta(\lambda)/k_B T] ds^{N_1} d\omega^{N_1} \dots ds^{N_n} d\omega^{N_n} dV \end{aligned} \quad (1)$$

where s^{N_i} are the configurations of the N_i molecules of type i , ω^{N_i} are the orientations and internal configurations of N_i molecules of type i , $U(s^N, \omega^N, \lambda)$ is the potential energy of the system, $\beta = 1/k_B T$, $\hat{q}_i(T)$ is the temperature dependent term in the molecular partition function for the molecule of type i , and $\eta(\lambda)$ are the biasing factors introduced to improve the probabilities of transitions in λ . The reader is referred to the Supporting Information for a detailed explanation of the molecular partition functions and partition functions of the osmotic ensemble.

From eq 1, it follows that the probability that the system is in a certain state is

$$\begin{aligned} p_{\text{biased}} \sim \exp \left[\beta \sum_{i=1}^n N_i \mu_i - \sum_{i=1}^n \ln N_i! + \sum_{i=1}^n N_i \ln(\hat{q}_i(T)V) \right. \\ \left. - \beta PV - \beta U(s^N, \omega^N, \lambda) \right] \exp[\eta(\lambda)/k_B T] \end{aligned} \quad (2)$$

This equation can be used to derive the acceptance rules in our Monte Carlo algorithm.

2.1.1. Reaction Ensemble Monte Carlo Using the Continuous Fractional Component Algorithm. Let us consider a reaction involving species c in a system consisting of n molecule types. For the species not involved in the reaction, the stoichiometric coefficient ν_i is set to 0 by definition. If a reaction takes place in the forward or reverse direction, there will be a change in the molecules of each component. The state before the reaction takes place is now denoted by old state “o”, whereas the state after the reaction takes place is denoted by new state “n”. Because the reaction has taken place, we know how the number of molecules of each component changes

$$N_{i,n} = N_{i,o} + \nu_i \quad (3)$$

The probabilities of existing in states “o” and “n” can be obtained from eq 2. Substituting eq 3 in eq 2 for the new state, the expressions for the probabilities to exist in the old and the new states are

$$\begin{aligned} p_{\text{o,biased}} \sim \exp \left[\beta \sum_{i=1}^n N_{i,o} \mu_i - \sum_{i=1}^n \ln N_{i,o}! + \sum_{i=1}^n N_{i,o} \ln(\hat{q}_i(T)V_o) \right. \\ \left. - \beta PV_o - \beta U_o(s^{N,o}, \omega^{N,o}, \lambda_o) \right] \exp[\eta(\lambda_o)/k_B T] \end{aligned} \quad (4)$$

$$p_{n,\text{biased}} \sim \exp \left[\beta \sum_{i=1}^n \nu_i \mu_i + \beta \sum_{i=1}^n N_{i,o} \mu_i - \sum_{i=1}^n \ln(N_{i,o} + \nu_i)! + \sum_{i=1}^n N_{i,o} \ln(\hat{q}_i(T) V_n) + \sum_{i=1}^n \nu_i \ln(\hat{q}_i(T) V_n) - \beta P V_n - \beta U_n(s^{N,n}, \omega^{N,n}, \lambda_n) \right] \exp[\eta(\lambda_n)/k_B T] \quad (5)$$

2.1.2. *Acceptance Rules in RxMC/CFC.* Averages in the Boltzmann ensemble (denoted by $\langle \dots \rangle$) follow directly from biased averages (denoted by $\langle \dots \rangle_{\text{biased}}$) according to⁴⁶

$$\langle A \rangle = \frac{\langle A \exp[-\eta(\lambda)] \rangle_{\text{biased}}}{\langle \exp[-\eta(\lambda)] \rangle_{\text{biased}}} \quad (6)$$

In the RxMC/CMC method, four types of trial moves are possible.

- (1) Change the position of a randomly selected molecule (either a regular or a fractional molecule).
- (2) Change the orientation of a randomly selected molecule (either a regular or a fractional molecule).
- (3) Change the volume of the system.
- (4) Change the coupling parameter λ of a randomly selected reaction chosen with equal probability that can be further divided into 3 cases ($\Delta\lambda$ is the change in λ)
 - (a) $0 \leq \lambda + \Delta\lambda \leq 1$.
 - (b) $\lambda + \Delta\lambda < 0$.
 - (c) $\lambda + \Delta\lambda > 1$.

The first two Monte Carlo moves are trivial and have the same acceptance rules as the ones derived previously.^{23,46} For the volume change Monte Carlo trial move, random walks are made in $\ln(V_n/V_{\text{ref}})$ ²³ in which V_{ref} is an arbitrary reference volume. The probabilities of existing in the old state “o” and the new state “n” are

$$p_{o,\text{biased}} \sim \beta P V_o \exp \left[\beta \sum_{i=1}^n N_{i,o} \mu_i - \sum_{i=1}^n \ln N_{i,o}! + \sum_{i=1}^n N_{i,o} \ln(\hat{q}_i(T) V_o) - \beta P V_o - \beta U_o(s^N, \omega^N, \lambda) \right] \exp[\eta(\lambda_o)/k_B T] \quad (7)$$

$$p_{n,\text{biased}} \sim \beta P V_n \exp \left[\beta \sum_{i=1}^n N_{i,o} \mu_i - \sum_{i=1}^n \ln N_{i,o}! + \sum_{i=1}^n N_{i,o} \ln(\hat{q}_i(T) V_n) - \beta P V_n - \beta U_n(s^N, \omega^N, \lambda) \right] \exp[\eta(\lambda_n)/k_B T] \quad (8)$$

For random walks in $\ln(V_n/V_{\text{ref}})$, $\lambda_o = \lambda_n$ and $\eta(\lambda_o) = \eta(\lambda_n)$. The acceptance rule is therefore

$$\text{acc}(o \rightarrow n) = \min \left(1, \left(\frac{V_n}{V_o} \right)^{N+1} \exp[-\beta P(V_n - V_o)] \exp[-\beta(U_n(s^N, \omega^N, \lambda) - U_o(s^N, \omega^N, \lambda))] \right) \quad (9)$$

This expression is the same as the acceptance rule derived previously.²³

We now consider the reaction move as a change in λ of the system for the reaction move, $V_o = V_n$. Looking in more detail at the three different cases when λ is changed as follows:

First case (a), where $0 \leq (\lambda + \Delta\lambda) \leq 1$, involves no addition or deletion of molecules. The old state is denoted by “o”, and λ_o

is the old coupling factor of the reaction. The new state is denoted by “n”, and $\lambda_n = \lambda_o + \Delta\lambda$. From eq 2, we can obtain the probabilities of existing in the old and new states. As the number of molecules in the system remain the same for the old and the new configurations, the acceptance rule is

$$\text{acc}(o \rightarrow n) = \min(1, \exp[-\beta(U_n(s^N, \omega^N, \lambda_n) - U_o(s^N, \omega^N, \lambda_o))] \exp[(\eta(\lambda_n) - \eta(\lambda_o))/k_B T]) \quad (10)$$

Second case (b), where $\lambda + \Delta\lambda > 1$, involves a reverse reaction. The λ of the old fractional reactant and product molecules are set to 1 and 0, respectively. New fractional reactant molecules are inserted into the system with $\lambda_n = (\lambda_o + \Delta\lambda) - 1$. Random product molecules are selected from the system, and their λ is set from 1 to $1 - \lambda_n$.

Third case (c), where $\lambda + \Delta\lambda < 0$, involves a forward reaction. The λ of the old fractional reactant and product molecules are set to 0 and 1, respectively. New fractional product molecules are inserted into the system with $\lambda_n = (\lambda_o + \Delta\lambda) - 1$. Random reactant molecules are selected from the system, and their λ is set to $1 - \lambda_n$.

In the second and third cases, the reaction has proceeded in either the reverse or forward direction, respectively. For a reaction involving n species, equilibrium is achieved when

$$\sum_{i=1}^n \nu_i \mu_i = 0 \quad (11)$$

Substituting eq 11 in eq 5, because the reaction takes place at equilibrium, the expression for the acceptance rule for the forward/reverse reaction (cases b and c) is

$$\text{acc}(o \rightarrow n) = \min \left(1, \prod_{i=1}^n \left(\frac{N_i^o!}{(N_i^o + \nu_i)!} (\hat{q}_i(T) V)^{\nu_i} \right) \exp[-\beta(U_n(s^N, \omega^N, \lambda_n) - U_o(s^N, \omega^N, \lambda_o))] \exp[(\eta(\lambda_n) - \eta(\lambda_o))/k_B T] \right) \quad (12)$$

The acceptance rule for the RxMC derived above for one reaction can be easily generalized to include many reactions in the same system. It is important to note that in the acceptance rule (eq 12) the volume term is included explicitly because during the simulation the volume of the system changes.

It is instructive to consider the case of a reaction in a mixture of ideal gases. In this case, the acceptance rule of eq 12 reduces to

$$\text{acc}(o \rightarrow n) = \min \left(1, \prod_{i=1}^n \left(\frac{N_i^o!}{(N_i^o + \nu_i)!} (\hat{q}_i(T) V)^{\nu_i} \right) \right) \quad (13)$$

If the total number of molecules does not change during the reaction ($\sum_{i=1}^n \nu_i = 0$), it is well-known from classical thermodynamics that the equilibrium constant is only a function of the molecular partition functions.⁴⁷ From eq 13, it can also be observed that there will be no dependence on the volume of the system when $\sum_{i=1}^n \nu_i = 0$, as the volume term V cancels out in eq 13 and the expression reduces to

$$\text{acc}(o \rightarrow n) = \min \left(1, \prod_{i=1}^n \left(\frac{N_i^o!}{(N_i^o + \nu_i)!} (\hat{q}_i(T))^{\nu_i} \right) \right) \quad (14)$$

If there is a change in the number of molecules during the reaction ($\sum_{i=0}^n \nu_i \neq 0$), the acceptance rule will now depend on the volume of the system, as can be seen from eq 13. It is important to consider the volume dependent term of the partition function explicitly in the acceptance rules because in many cases the number of molecules during the reaction changes ($\sum_{i=0}^n \nu_i \neq 0$). It is unclear whether this volume term was taken into account correctly in previous studies from the literature. Of course, the final results will not be affected if the simulations consider reactions where the number of molecules does not change due to the reaction.^{28–30}

2.2. Simulation Details. Two different sets of reactions are studied to obtain the equilibrium speciations by including: (1) reactions R1–R4 and (2) only reaction R5. All simulations are performed in the Reaction Monte Carlo Ensemble (RxMC) in the constant temperature, constant pressure ensemble. The hydrostatic pressure of the system equals 1 bar. The effect of temperature on the equilibrium compositions of the mixture and different loadings of CO₂ are also investigated. The initial concentration of MEA in the aqueous MEA solution is 30 wt %. Boettinger et al.⁹ measured the speciations at different loadings higher than 0.5 mol CO₂/mol MEA using online NMR spectroscopy. To achieve high loadings of CO₂ in experiments, the partial pressure of CO₂ ranged from 5 to 25 bar. In our simulations, a system with a fixed number of CO₂ molecules is simulated and only the hydrostatic pressure of the system needs to be specified. As the properties of a liquid phase do not depend much on the hydrostatic pressure, and the total loading of CO₂ is specified, a hydrostatic pressure of 1 bar can be safely assumed.

Quantum mechanical simulations using GAUSSIAN 09⁴⁸ are performed to obtain the partition functions \hat{q}_i of the isolated molecules required for the RxMC/CFC molecular simulations. All molecular species involved in the reaction were optimized with a second order Møller–Plesset perturbation method (MP2) in combination with a 6-311+G(2d,2p) basis set at temperature of 293, 333, and 353 K. Frequency analysis was performed on the optimized geometries to confirm the true minima on the potential energy surface and to obtain partition functions of all of the molecules. All of the calculations were performed with GAUSSIAN 09.⁴⁸ Mulliken atomic charges were obtained from population analysis of a self-consistent field density matrix. The individual contributions of translational, vibrational, rotational, and electronic motions are considered for the calculation of the partition function for every molecule.⁴⁹ The partition functions were split into temperature- and volume-dependent parts (details are provided in the Supporting Information). The values of the computed partition functions of the molecules at different temperatures are listed in the Supporting Information.

Force fields for the MEA have been taken from the OPLS force field.⁵⁰ Intermolecular and intramolecular potential parameters for MEACOO[−] and MEAH⁺ have also been taken from the OPLS force field. Force field parameters for CO₂ have been taken from the TraPPE force field,⁵¹ and for water, the Tip4p water model has been used.⁵² The force field parameters for H₃O⁺ are taken from Vacha et al.⁵³ The force field parameters for HCO₃[−] and CO₃^{2−} have been taken from the OPLS database. Water, MEA, MEA⁺, MEACOO[−], H₃O⁺, HCO₃[−], and CO₃^{2−} are modeled as rigid molecules. The partial charges for HCO₃[−], CO₃^{2−}, MEACOO[−], and MEAH⁺ have been computed from quantum mechanical simulations in GAUSSIAN 09.⁴⁸ The force field parameters for all of the species are

specified in the Supporting Information. Electrostatic interactions were handled by the Ewald summation algorithm⁵⁴ with a relative precision of 10^{−5}. The cutoff radius was set at 12 Å for the Lennard-Jones interactions. The Lennard-Jones (LJ) parameters are σ and ϵ .⁵⁵ The Lorentz–Berthelot mixing rules were used to calculate the Lennard-Jones parameters between different atoms (σ_{ij} and ϵ_{ij}). Monte Carlo simulations in the RxMC/CFC ensemble were performed using RASPA,⁵⁵ a program for Monte Carlo and molecular dynamics simulations. Monte Carlo simulations of 1 million cycles were performed for equilibration, and production runs of 2 million cycles were performed, where one MC cycle is equal to the total number of molecules in the system. The probabilities of selecting a translation move, a rotation move, a partial reinsertion move, and a reaction move were all 0.245. The probability of selecting a volume change move was 0.02. Simulations were performed with 444 water molecules, 56 MEA molecules, and the appropriate number of CO₂ molecules depending on the loading. The size of the simulation box varied around 27 Å. By switching off electrostatics and intermolecular van der Waals interactions, the effects of electrostatics and intermolecular interactions on the reaction equilibrium were studied. At the start of the simulation, fractional molecules were assigned for all reacting species for both reactants and products in reactions R1–R4. The net charge of the fractional molecules (both the reactants and products) of reactions R1–R4 is not zero. It is important to note that if we sum reactions R1–R4, the total net charge of the reactants equals −1. Similarly, the total net charge of products of the summed reactions also equals −1. To keep the simulation box charge neutral, independent of the value of λ for each reaction, two H₃O⁺ fractional molecules, one as a reactant and the other as a product in reaction R2, were added to the simulation box. This ensures that during the reaction the simulation box is always charge neutral. For the RxMC/CFC, the Lennard-Jones parameters as well as the partial charges are scaled with a pseudo coupling factor, which is changed during the reaction move. The scaled Lennard-Jones and electrostatic potentials are specified in detail in the Supporting Information.

3. RESULTS AND DISCUSSION

3.1. Effects of Electrostatics and Intermolecular van der Waals Interactions. When there are no intermolecular interactions between molecules, the system behaves as an ideal gas. For an ideal gas system, the equilibrium constant can be written directly in terms of the molecular partition functions of the individual species,⁵⁶ which can be calculated from quantum simulations. A detailed derivation of this is provided in the Supporting Information.

To observe the effect of intermolecular interactions, we “switched off” the intermolecular van der Waals interactions and electrostatics (i.e., all of the intermolecular Lennard-Jones parameters and electrostatics were set to zero). From the simulations, it was observed that forward reactions did not take place when including (1) reactions R1–R4 and (2) only reaction R5. Equilibrium constants for these ideal gas reactions calculated from quantum simulations are specified in the Supporting Information. The equilibrium constants for the forward reaction are extremely low. Equilibrium concentrations of the species for the ideal gas system can be obtained by solving the nonlinear expressions for the equilibrium constants. The analytical solutions yield extremely low concentrations of carbamates and protonated amines. This is consistent with the

results obtained from simulations performed when the intermolecular van der Waals interactions and the electrostatics are set to zero. It can be observed from the results of the simulations and analytical solutions that intermolecular interactions are necessary to compute the equilibrium concentrations of the species. Equilibrium speciations cannot be obtained by only performing quantum simulations, as the system cannot be treated as an ideal gas. As expected, solvation of the ions in the solution is essential for the different reactions to take place. Classical simulations take into account the intermolecular interactions between the species, and this is necessary to compute the equilibrium concentrations of the species. If the reaction occurs in the ideal gas phase, the ions are not solvated, and this is energetically very unfavorable.

3.2. Chemical Equilibrium of Reactions R1–R4 and R5.

The equilibrium mole fractions of the different species were obtained at temperature of 293, 333, and 353 K and at a hydrostatic pressure of 1 bar for different loadings of CO_2 (mol CO_2 /mol MEA) by performing RxMC/CMC. In Figures 1, 2,

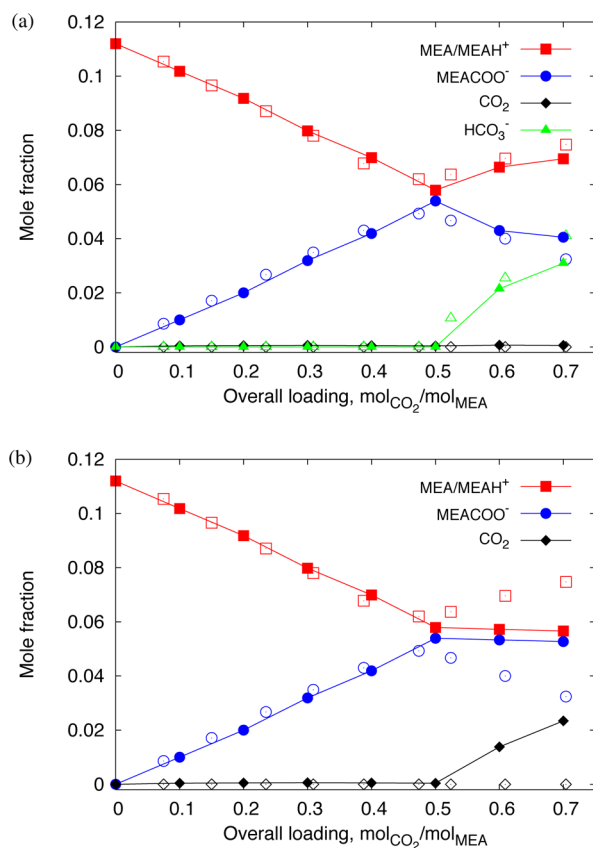


Figure 1. Mole fractions of MEA/MEA⁺ (squares), MEACOO[−] (circles), CO₂ (diamonds), and HCO₃[−] (triangles) for 30 wt % aqueous MEA solutions at $T = 293$ K. The open symbols are the results from experiments.⁹ The closed symbols are the results obtained from the RxMC/CFC simulations (a) including reactions R1–R4 and (b) including only reaction R5. The lines are added for clarity.

and 3, the equilibrium mole fractions of the species MEA, MEAH⁺, MEACOO[−], CO₂, and HCO₃[−] are compared to experimental data.^{9,22} Poplsteinova et al.²² and Boettinger et al.⁹ measured the equilibrium speciation of a CO₂/MEA/H₂O system using NMR spectroscopy. Boettinger et al.⁹ report the sum of equilibrium concentrations of MEA and MEAH⁺, because it was impossible to distinguish between the

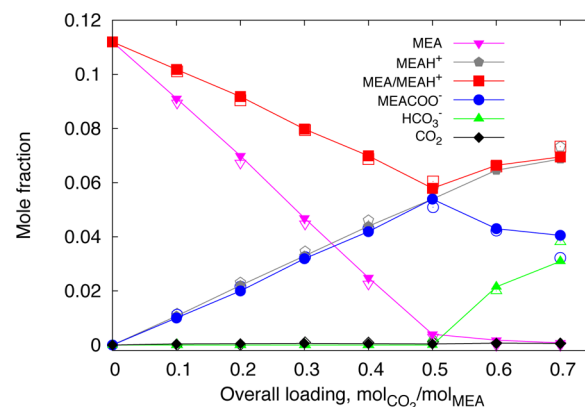


Figure 2. Mole fractions of MEA (inverted triangles), MEAH⁺ (pentagons), MEA/MEA⁺ (squares), MEACOO[−] (circles), CO₂ (diamonds), and HCO₃[−] (triangles) for 30 wt % aqueous MEA solutions at $T = 293$ K. The open symbols are results from the thermodynamic model combined with experimental data.⁹ The closed symbols are results obtained from the RxMC/CFC simulations including reactions R1–R4. The lines added for clarity.

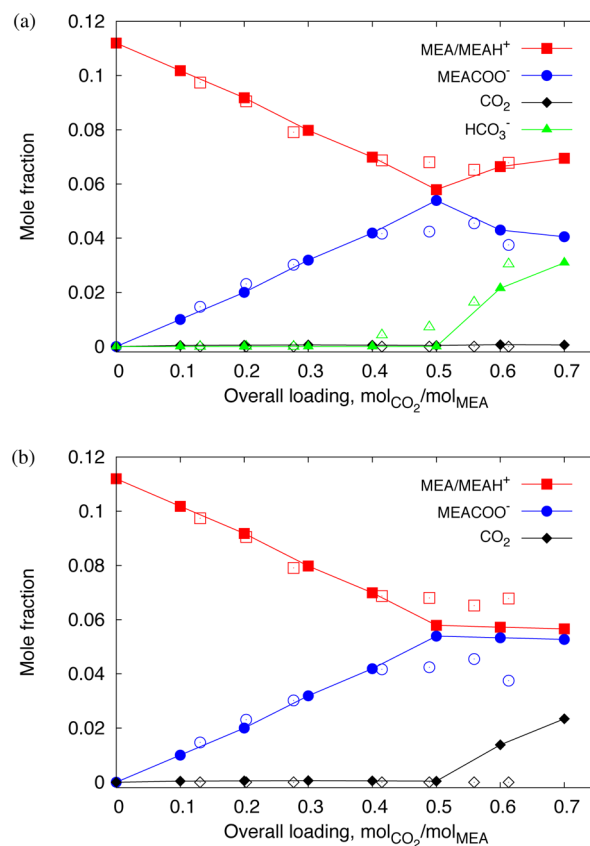


Figure 3. Mole fractions of MEA/MEA⁺ (squares), MEACOO[−] (circles), CO₂ (diamonds), and HCO₃[−] (triangles) for 30 wt % aqueous MEA solutions at $T = 333$ K. The open symbols are results from experiments.⁹ The closed symbols are the results obtained from the RxMC/CFC simulations (a) including reactions R1–R4 (b) including only reaction R5. The lines are a guide to the eye.

protonated and unprotonated MEA experimentally. To obtain the individual equilibrium concentrations of MEA and MEAH⁺, these authors used a thermodynamic model (see below).

Figure 1a shows the speciation of the CO₂/MEA solution for different loadings of CO₂ (mol CO₂/mol MEA) at 293 K and 1

bar when reactions R1–R4 are used. The equilibrium concentration of the different species of the CO_2/MEA solution exhibits behavior typical of primary amines. From low loadings to 0.5 mol CO_2/mol MEA, all CO_2 molecules react with the MEA molecules, forming the carbamate and protonated amine products. The concentrations of the carbamate and the protonated MEA increase as the loading of CO_2 increases until 0.5 mol CO_2/mol MEA, whereas the concentration of MEA decreases. At a CO_2 loading of 0.5 mol CO_2/mol MEA, all of the MEA has now reacted with the CO_2 . Beyond loadings of CO_2 of 0.5 mol CO_2/mol MEA, the concentrations of the carbamate start to decrease, and the concentrations of the protonated MEA increase. Beyond the loadings of CO_2 of 0.5 mol/mol MEA, bicarbonate ions were observed. The simulation results are in excellent agreement with the experimental results of Boettinger et al.⁹

Figure 1b shows the equilibrium concentrations of MEA, MEA^+ , MEACOO^- , and CO_2 for different loadings of CO_2 (mol CO_2/mol MEA) at 293 K and 1 bar when only reaction R5 is considered. The results of equilibrium speciations obtained from simulating only reaction R5 follow the same trends for the concentrations of MEA, protonated MEA, and the carbamate as they did when we included reactions R1–R4. Up to loadings of 0.5 mol CO_2/mol MEA, the concentrations of the carbamate and protonated MEA increase, and the concentration of free MEA decreases. Beyond loadings of 0.5 mol CO_2/mol MEA, all of the MEA has typically reacted with the CO_2 . The concentrations of MEA, protonated MEA, and MEACOO^- remain constant, whereas the concentration of unreacted CO_2 increases for loadings higher than 0.5 mol CO_2/mol MEA.

Boettinger et al.⁹ also used a thermodynamic model to study the $\text{CO}_2/\text{MEA}/\text{H}_2\text{O}$ system and obtained the individual equilibrium concentrations of the MEA, MEA^+ , MEACOO^- , CO_2 , and HCO_3^- species. These authors developed their model by simultaneously taking into consideration the chemical reactions and the vapor–liquid equilibria of the $\text{CO}_2/\text{MEA}/\text{H}_2\text{O}$ mixture. Figure 2 compares our simulation results of the individual equilibrium concentrations including MEA and MEA^+ with the results from the thermodynamic model of Boettinger et al. We find an excellent agreement with the model. It is important to note that we obtained individual concentrations of all of the species in the mixture directly from simulations, and we did not need to use any iterative modeling technique that requires binary interaction parameters, activity coefficients of molecular and ionic species, equilibrium coefficients, or so forth as inputs.

Figures 3 and 4 show the results of the speciations at 333 and 353 K and 1 bar. It can be observed that an increase in temperature does not significantly affect the equilibrium concentrations of the species. For Figure 4, there is no experimental data beyond loadings of 0.5 mol CO_2/mol MEA. This is again in excellent agreement with the experimental results of Boettinger et al.,⁹ who also observed that the speciations of the CO_2/MEA solution are only very weakly dependent on temperature.

4. CONCLUSIONS

Monte Carlo simulations in the Reaction Ensemble using a continuous fractional component method provide an excellent description of the equilibrium concentrations of all relevant species in the chemisorption of CO_2 in MEA/water solutions. The simulations were performed at different temperatures, and

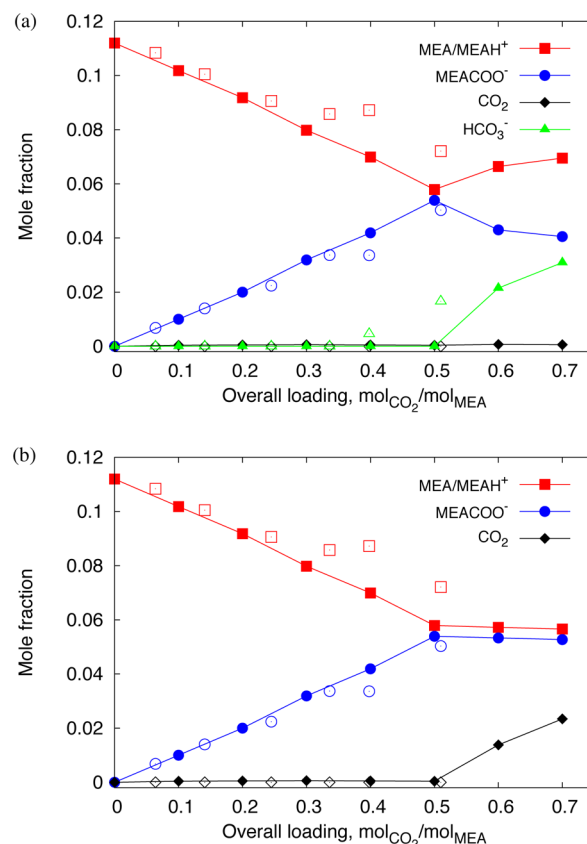


Figure 4. Mole fractions of MEA/MEA^+ (squares), MEACOO^- (circles), CO_2 (diamonds), and HCO_3^- (triangles) for 30 wt % aqueous MEA solutions at $T = 353$ K. The open symbols are results from experiments.⁹ The closed symbols are the results obtained from the RxMC/CFC simulations (a) including reactions R1–R4 and (b) including only reaction R5. The lines are added for clarity.

the results from the simulations are in excellent agreement with the experimental results. Equilibrium concentrations of MEA, MEA^+ , MEACOO^- , and CO_2 from reactions R1–R4 and R5 are identical for loadings up to 0.5 mol CO_2/mol MEA; beyond that, they are different. For accurate results of loadings in excess of 0.5 mol CO_2/mol MEA to be obtained, reactions R1–R4 must be included in the simulation. This RxMC/CFC methodology opens possibilities for investigating the effects of the solvents in the reactions. Chemisorption of CO_2 in different solvents can be studied computationally to obtain the equilibrium concentrations. Only the thermodynamics need to be considered, and the different transition states and reaction pathways can be ignored. This method may also be used to investigate the effect of the chemistry of amines, for example, for the addition of different functional groups.^{14,16}

■ ASSOCIATED CONTENT

Supporting Information

Information on the force field parameters, detailed explanation of the molecular partition functions, and the derivation of the partition function for the osmotic ensemble with continuous fractional component Monte Carlo. The Supporting Information is available free of charge on the ACS Publications website at DOI: 10.1021/acs.jctc.5b00160.

■ AUTHOR INFORMATION

Corresponding Author

*E-mail: t.j.h.vlugt@tudelft.nl.

Notes

The authors declare no competing financial interest.

■ ACKNOWLEDGMENTS

This work was performed as a part of the CATO-2 program, the Dutch National R&D program on CO₂ capture, transport, and storage, funded by the Dutch Ministry of Economic Affairs. This work was also supported by NWO Exacte Wetenschappen (Physical Sciences) for the use of supercomputer facilities with financial support from the Nederlandse Organisatie voor Wetenschappelijk Onderzoek (Netherlands Organization for Scientific Research, NWO). This work is also supported by The Netherlands Research Council for Chemical Sciences (NWO/CW) through a VIDI grant (D.D.).

■ REFERENCES

- (1) Meinshausen, M.; Meinshausen, N.; Hare, W.; Raper, S. C. B.; Frieler, K.; Knutti, R.; Frame, D. J.; Allen, M. R. *Nature* **2009**, *458*, 1156–1162.
- (2) Solomon, S. *Proc. Natl. Acad. Sci. U.S.A.* **2009**, *106*, 1704–1709.
- (3) Metz, B.; Davidson, O.; de Coninck, H.; Loos, M.; Meyer, L. *Carbon Dioxide Capture and Storage: Special Report of the Intergovernmental Panel on Climate Change*; Cambridge University Press: Cambridge, 2005.
- (4) Puxty, G.; Rowland, R.; Allport, A.; Yang, Q.; Bown, M.; Burns, R.; Maeder, M.; Attalla, M. *Environ. Sci. Technol.* **2009**, *43*, 6427–6433.
- (5) D'Alessandro, D. M.; Smit, B.; Long, J. R. *Angew. Chem., Int. Ed.* **2010**, *49*, 6058–6082.
- (6) Abu-Zahra, M. R. M.; Schneiders, L. H. J.; Niederer, J. P. M.; Feron, P. H. M.; Versteeg, G. F. *Int. J. Greenhouse Gas Control* **2007**, *1*, 37–46.
- (7) Rochelle, G. T. *Science* **2009**, *325*, 1652–1654.
- (8) Jou, F.; Mather, A. E.; Otto, F. D. *Can. J. Chem. Eng.* **1995**, *73*, 140–147.
- (9) Boettinger, W.; Maiwald, M.; Hasse, H. *Fluid Phase Equilib.* **2008**, *263*, 131–143.
- (10) Khakharia, P.; Brachert, L.; Mertens, J.; Huizinga, A.; Schallert, B.; Schaber, K.; Vlugt, T. J. H.; Goetheer, E. L. V. *Int. J. Greenhouse Gas Control* **2013**, *19*, 138–144.
- (11) Khakharia, P.; Kvamsdal, H. M.; da Silva, E. F.; Vlugt, T. J. H.; Goetheer, E. L. V. *Int. J. Greenhouse Gas Control* **2014**, *28*, 57–64.
- (12) Khakharia, P.; Huizinga, A.; Lopez, C. J.; Sanchez, C. S.; de Miguel Mercader, F.; Vlugt, T. J. H.; Goetheer, E. L. V. *Ind. Eng. Chem. Res.* **2014**, *53*, 13195–13204.
- (13) Chen, Q.; Balaji, S. P.; Ramdin, M.; Gutierrez-Sevillano, J. J.; Bardow, A.; Goetheer, E. L. V.; Vlugt, T. J. H. *Ind. Eng. Chem. Res.* **2014**, *53*, 18081–18090.
- (14) Gangarapu, S.; Marcelis, A. T. M.; Zuilhof, H. *ChemPhysChem* **2012**, *13*, 3973–3980.
- (15) Danckwerts, P. V. *Chem. Eng. Sci.* **1979**, *34*, 443–446.
- (16) Gangarapu, S.; Marcelis, A. T. M.; Zuilhof, H. *ChemPhysChem* **2013**, *14*, 3936–3943.
- (17) Manzolini, G.; Fernandez, E. S.; Rezvani, S.; Macchi, E.; Goetheer, E. L. V.; Vlugt, T. J. H. *Appl. Energy* **2014**, *138*, 546–558.
- (18) Ramdin, M.; de Loos, T. W.; Vlugt, T. J. H. *Ind. Eng. Chem. Res.* **2012**, *51*, 8149–8177.
- (19) Sartori, G.; Savage, G. W. *Ind. Eng. Chem. Res.* **1983**, *22*, 239–249.
- (20) Batt, W. T.; Maddox, R. N.; Mains, G. J.; Rahman, M.; Vaz, R. N. *Gas Conditioning Conference*; University of Oklahoma: Norman, Oklahoma, 1980.
- (21) Maddox, R. N.; Mains, G. J.; Rahman, M. *Ind. Eng. Chem. Res.* **1987**, *26*, 27–31.
- (22) Jakobsen, J. P.; Krane, J.; Svendsen, H. F. *Ind. Eng. Chem. Res.* **2005**, *44*, 9894–9903.
- (23) Frenkel, D.; Smit, B. *Understanding Molecular Simulation, From Algorithms to Applications*, 2nd ed.; Academic Press, London, U.K., 2002.
- (24) Car, R.; Parinello, M. *Phys. Rev. Lett.* **1985**, *55*, 2471–2474.
- (25) van Duin, A. C.; Dasgupta, S.; Lorant, F.; Goddard, W. A., III. *J. Phys. Chem. A* **2001**, *105*, 9396–9409.
- (26) Johnson, J. K.; Panagiotopoulos, A. Z.; Gubbins, K. E. *Mol. Phys.* **1994**, *81*, 717–733.
- (27) Smith, W. R.; Triska, B. J. *Chem. Phys.* **1994**, *100*, 3019–3027.
- (28) Hansen, N.; Jakobtorweihen, S.; Keil, F. J. *J. Chem. Phys.* **2005**, *122*, 1–11.
- (29) Jakobtorweihen, S.; Hansen, N.; Keil, F. J. *J. Chem. Phys.* **2006**, *125*, 1–9.
- (30) Rosch, T. W.; Maginn, E. J. *J. Chem. Theory Comput.* **2011**, *7*, 269–279.
- (31) Turner, C. H.; Johnson, J. K.; Gubbins, K. E. *J. Chem. Phys.* **2001**, *114*, 1851–1859.
- (32) Carrero-Mantilla, J.; Llano-Restrepo, M. *Fluid Phase Equilib.* **2004**, *219*, 181–193.
- (33) Lisal, M.; Nezbeda, I.; Smith, W. R. *J. Chem. Phys.* **1999**, *110*, 8597–8604.
- (34) Lisal, M.; Brennan, J. K.; Smith, W. R. *J. Chem. Phys.* **2006**, *124*, 064712.
- (35) Lisal, M.; Smith, W. R.; Nezbeda, I. *AIChE J.* **2000**, *46*, 866–875.
- (36) Lisal, M.; Smith, W. R.; Nezbeda, I. *J. Phys. Chem. B* **1999**, *103*, 10496–10505.
- (37) Shi, W.; Maginn, E. J. *J. Chem. Theory Comput.* **2007**, *3*, 1451–1463.
- (38) Torres-Knoop, A.; Balaji, S. P.; Vlugt, T. J. H.; Dubbeldam, D. *J. Chem. Theory Comput.* **2014**, *10*, 942–952.
- (39) Shi, W.; Maginn, E. J. *J. Comput. Chem.* **2008**, *29*, 2520–2530.
- (40) Balaji, S. P.; Schnell, S. K.; McGarrity, E. S.; Vlugt, T. J. H. *Mol. Phys.* **2013**, *111*, 285–294.
- (41) Balaji, S. P.; Schnell, S. K.; Vlugt, T. J. H. *Theor. Chem. Acc.* **2013**, *132*, 1–8.
- (42) Schnell, S. K.; Englebienne, P.; Simon, J. M.; Kruger, P.; Balaji, S. P.; Kjølstrup, S.; Bedeaux, D.; Bardow, A.; Vlugt, T. J. H. *Chem. Phys. Lett.* **2013**, *582*, 154–157.
- (43) Polderman, L. D.; Dillon, C. P.; Steele, A. B. *Oil Gas J.* **1955**, *53*, 180–183.
- (44) Strazisar, B. R.; Anderson, R. R.; White, C. M. *Energy Fuels* **2003**, *17*, 1034–1039.
- (45) Turner, C. H.; Brennan, J. K.; Lisal, M.; Smith, W. R.; Johnson, J. K.; Gubbins, K. E. *Mol. Sim.* **2008**, *34*, 119–146.
- (46) Allen, M. P.; Tildesley, D. J. *Computer Simulation of Liquids*; Oxford University Press: U.S.A., 1989.
- (47) Mayer, J. E.; Mayer, M. G. *Statistical Mechanics*; Wiley: New York, 1963.
- (48) Frisch, M. J.; Trucks, G. W.; Schlegel, H. B.; Scuseria, G. E.; Robb, M. A.; Cheeseman, J. R.; Scalmani, G.; Barone, V.; Mennucci, B.; Petersson, G. A.; Nakatsuji, H.; Caricato, M.; Li, X.; Hratchian, H. P.; Izmaylov, A. F.; Bloino, J.; Zheng, G.; Sonnenberg, J. L.; Hada, M.; Ehara, M.; Toyota, K.; Fukuda, R.; Hasegawa, J.; Ishida, M.; Nakajima, T.; Honda, Y.; Kitao, O.; Nakai, H.; Vreven, T.; Montgomery, J. A., Jr.; Peralta, J. E.; Ogliaro, F.; Bearpark, M.; Heyd, J. J.; Brothers, E.; Kudin, K. N.; Staroverov, V. N.; Kobayashi, R.; Normand, J.; Raghavachari, K.; Rendell, A.; Burant, J. C.; Iyengar, S. S.; Tomasi, J.; Cossi, M.; Rega, N.; Millam, J. M.; Klene, M.; Knox, J. E.; Cross, J. B.; Bakken, V.; Adamo, C.; Jaramillo, J.; Gomperts, R.; Stratmann, R. E.; Yazyev, O.; Austin, A. J.; Cammi, R.; Pomelli, C.; Ochterski, J. W.; Martin, R. L.; Morokuma, K.; Zakrzewski, V. G.; Voth, G. A.; Salvador, P.; Dannenberg, J. J.; Dapprich, S.; Daniels, A. D.; Farkas, A.; Foresman, J. B.; Ortiz, J. V.; Cioslowski, J.; Fox, D. J. *GAUSSIAN 09*, revision D.01; Gaussian Inc.: Wallingford, CT, 2009.

- (49) Ochterski, J. W. Thermochemistry in Gaussian. http://www.gaussian.com/g_whitepap/thermo/thermo.pdf (accessed January 3, 2015).
- (50) Rizzo, R. C.; Jorgensen, W. L. *J. Am. Chem. Soc.* **1999**, *121*, 4827–4836.
- (51) Potoff, J. J.; Siepmann, J. I. *AIChE J.* **2001**, *47*, 1676–1682.
- (52) Jorgensen, W. L.; Chandrasekhar, J.; Madura, J. D.; Impey, R. W.; Klein, M. L. *J. Chem. Phys.* **1983**, *79*, 926–935.
- (53) Vacha, R.; Buch, V.; Milet, A.; Devlind, J. P.; Jungwirth, P. *Phys. Chem. Chem. Phys.* **2007**, *9*, 4736–4747.
- (54) Ewald, P. P. *Ann. Phys.* **1921**, *64*, 253–287.
- (55) Dubbeldam, D.; Calero, S.; Ellis, D. E.; Snurr, R. Q. *Mol. Sim.* **2015**, DOI: 10.1080/08927022.2015.1010082.
- (56) Hill, T. L. *An Introduction to Statistical Thermodynamics*; Dover Books: New York, 1987.